A Novel Interference Rejection Method for GPS Receivers

M. Pashaian*, M. R. Mosavi*(C.A.), M. S. Moghaddasi* and M. J. Rezaei*

Abstract: This paper proposes a new method for rejecting the Continuous Wave Interferences (CWI) in the Global Positioning System (GPS) receivers. The proposed filter is made by cascading an adaptive Finite Impulse Response (FIR) filter and a Wavelet Packet Transform (WPT) based filter. Although adaptive FIR filters are easy to implement and have a linear phase, they create self-noise in the rejection of strong interferences. Moreover, the WPT which provides detailed signal decomposition can be used for the excision of single-tone and multi-tone CWI and also for de-noising the retrieved GPS signal. By cascading these two filters, the self-noise imposed by FIR filter and the remaining jamming effects on GPS signal can be eliminated by the WPT based filter. The performance analysis of the proposed cascade filter is presented in this paper and it is compared with the FIR and the WPT based filters. Experimental results illustrate that the proposed method offers a better performance under the interference environments of interest in terms of the signal-to-noise ratio gain and mean square error factors compared to previous methods.

Keywords: Cascade Filter, Interference Rejection, Notch Filter, Wavelet Packet Transform.

1 Introduction

Global Positioning System (GPS) satellites use Direct Sequence Spread Spectrum (DSSS) for transmitting the navigation data. The signals coming from the GPS satellites are so weak. That it is easy for an intentional interference to overcome the inherent system's anti-jamming ability. Although DSSS systems have the inherent ability to eliminate low-power intentional interferences (e.g. jammers) and unintentional interferences, they cannot tolerate high-power ones [1, 2]. Therefore, it is necessary to apply additional techniques for improving the receiver anti-jamming performance. Continuous Wave Interference (CWI) is one of the most common types of interference signals in the GPS [3]. Hence, in this paper the mitigation technique of CWI is investigated.

Narrowband interference rejection techniques include adaptive filtering, time-frequency methods and adaptive antennas [1-4]. Adaptive antennas can be employed for mitigation of both narrowband and wideband jammers, but they are computationally complex [5, 6]. Time-frequency domain techniques [7, 8], like Short Time Fourier Transform (STFT) based processing [9, 10], filter banks [11], Wavelet Transform (WT) [12-14] and subspace processing [15, 16] are well suited for low cost and low power applications [8, 13]. These techniques study a signal in both time and frequency domains simultaneously. Since GPS signals are low power wideband signals, the narrowband jamming can be easily distinguished from the GPS signal [8, 9]. The STFT and the filter bank use fixed windows; therefore, they are not proper for processing the non-stationary signals. However, they have advantages such as minimum signal distortion, low power, and low cost implementation. In the wavelet analysis, the use of scalable modulated window solves the signal-cutting problem of STFT and the filter bank and provides a flexible resolution in both time and frequency domains [12-14].

Adaptive filtering techniques like Adaptive Notch Filters (ANFs) [17-20], Kalman filter [21, 22], Approximate Conditional Mean (ACM) filter [23] and Augmented State ACM (ASACM) filter [24] attempt to minimize the error of a predictor output using techniques such as least mean squares algorithm and adjust their parameters to optimize a cost function. Adaptive filtering can be used in low power, low cost, and small size applications. However, without prior knowledge of the jamming model parameters, Kalman and ACM filters do not have acceptable performances.

Iranian Journal of Electrical & Electronic Engineering, 2016.
Paper received 10 October 2015 and accepted 23 January 2016.
* The Authors are with the Department of Electrical Engineering, Iran University of Science and Technology, Tehran, Iran.
E-mails: Pashaian@elec.iust.ac.ir, M_Mosavi@iust.ac.ir, Salamat1989@elec.iust.ac.ir and Mj_rezaei@iust.ac.ir.

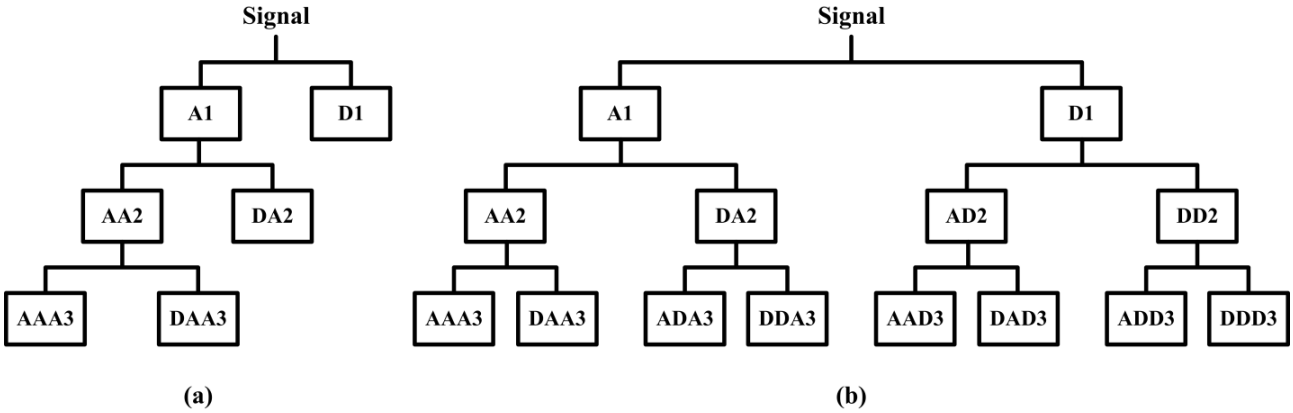

Fig. 1 Decomposition tree of the (a) DWT and (b) WPT.

Furthermore, computational complexity of the ASACM filter increases exponentially for the rejection of Multi-Tone CWI (MCWI) [17-24].

The WT shows a good performance for the rejection of narrowband or linear chirp interference [14], but its performance degrades for very narrowband or CW interferences mitigation. In the later cases, the number of decomposition levels and also computational complexity increases. So, notch filters may be preferred for the rejection of CWI [18-20].

In the notch filtering method, the Instantaneous Frequency (IF) of the interference is used to construct a time-varying notch filter that removes the interference. With comparing notch filtering with other interference suppression techniques, it has the lowest cost, and appropriate CWI rejection, and it is computationally efficient. Hence, it is suitable to be implemented in a GPS software receiver. However, this method also causes undesirable distortions in the signal and produce self-noise that is effective in the reduction of receiver Signal-to-Noise power Ratio (SNR), especially in high power interference cases [17].

The Wavelet Packet (WP) method is a generalization of wavelet decomposition that offers a richer signal analysis. In the Wavelet Packet Transform (WPT), both high and low frequency bands are processed. Therefore, WPT results the uniform frequency bands division [12, 14]. This property is useful for the interference rejection applications.

The main idea of this paper is cascading an adaptive Finite Impulse Response (FIR) notch filter with an adaptive WPT based filter to overcome their drawbacks. The use of adaptive WPT based filter overcomes noise effect of notch filter and removes the remaining interference effect. On the other hand, as the main portion of jamming signal is mitigated by the ANF, the number of WPT decomposition levels will be decreased. The cascade filter is implemented in a GPS software receiver to mitigate the CWI.

This paper is organized as follows. In the section 2, the theoretical concepts of WT and WPT are expressed. An introduction of the received signal structure, ANF and adaptive WPT filter are presented in section 3. In this section, the proposed jamming mitigation technique based on cascading notch filter and WPT based filter is also described. In section 4, the test results and the performance evaluation of the proposed method in different jamming scenarios are presented. Finally, the conclusion is given in section 5.

2 Wavelet Transform

Wavelets are mathematical functions that decompose data into different frequency components. Decomposition process can be done in different scales and any components of these scales can be studied separately. WT is a mathematical tool which provides both time and frequency information of a sequence of data. So, this property is useful for non-stationary signal processing [12-14].

2.1 Wavelet Packet Transform

The process of WPT is similar to the Discrete Wavelet Transform (DWT). According to Fig. 1 in the DWT, a signal is split into low frequency (approximation) and high frequency (detail) parts. Then, the approximation part is decomposed into another low and high frequency parts. However, in WPT the detail parts are also decomposed to the approximation and detail parts at each level [12].

In the anti-jamming applications which the information of both low and high frequency components are important and a higher frequency resolution is needed, the WPT is a better choice than the DWT. WP is described as:

$$\psi^{i}_{j,k}(t)=2^{-j/2}\psi^{i}(2^{-j}t-k) \quad (1)$$

where i is the frequency band parameter, j and k are the scale and translation parameters, respectively. The wavelet is obtained by:

$$\psi^{2i}(t)=\frac{1}{\sqrt{2}}\sum_{k=-\infty}^{\infty}h(k)\psi^{i}\left(\frac{t}{2}-k\right) \quad (2)$$

$$\psi^{2i+1}(t)=\frac{1}{\sqrt{2}}\sum_{k=-\infty}^{\infty} g(k)\psi^{i}\left(\frac{t}{2}-k\right)a \quad (3)$$

Wavelets are the scaled and translated versions of a mother wavelet $\psi(t)$. The coefficients $g(k)$ and $h(k)$ form a high pass filter (wavelet filter) and a low pass filter (scale filter), respectively. The WP coefficients C of the signal $f(t)$ can be calculated as:

$$C^{i}_{j,k}=\int_{-\infty}^{\infty} f(t)\psi^{i}_{j,k}(t)dt \quad (4)$$

Then the WP component of the signal at a certain node can be calculated as:

$$f^{i}_{j}(t)=\sum_{k=-\infty}^{\infty} C^{i}_{j,k}\psi^{i}_{j,k}(t)dt \quad (5)$$

Finally, the original signal can be obtained by the summation of all WP components at jth level:

$$f(t)=\sum_{i=1}^{2i} f^{i}_{j}(t) \quad (6)$$

3 Proposed Rejection Technique

3.1 Received Signal Model

The received spread spectrum GPS signal $y(t)$ can be represented as:

$$y(t)=s(t)+n(t)+\sum_{k=1}^{K} j_k(t)=s(t)+n(t)+j(t) \quad (7)$$

where $n(t)$ is the additive white Gaussian noise and $j(t)$ is the total jamming signal which is made by different jammers $j_k(t)$. $s(t)$ represents the transmitted spread spectrum GPS signal and it is described as:

$$s(t)=[D(t)\oplus CA(t)]\cos(2\pi f_{L1}t) \quad (8)$$

where $CA(t)$ is the coarse/acquisition (C/A) code sequence with chip rate 1.023 MHz and $D(t)$ is the transmitted baseband navigation data which is in binary form (±1) with duration T = 20 msec. f_{L1} is the GPS L1 carrier frequency (f_{L1} = 1575.42 MHz). It is to be noted that in this paper, the jamming signal is a combination of CW jammers $j_k(t)$:

$$j_k(t)=A\sin(\omega_0 t+\varphi) \quad (9)$$

where A, ω_0 and φ are the jamming amplitude, frequency and phase, respectively.

3.2 Adaptive Notch Filter

A notch filter based anti-jamming technique concentrates on the suppression of the high spectral peaks related to the interferences. A notch filter is defined as a filter that passes all frequencies except those in a stop-band band. A three coefficient ANF that can suppress a single CWI is introduced as [17]:

$$H(z)=z^{-1}(z-ae^{-j\omega_0})(1-az^{-1}e^{j\omega_0}) \quad (10)$$

where a is a parameter that controls the depth of the notch filter.

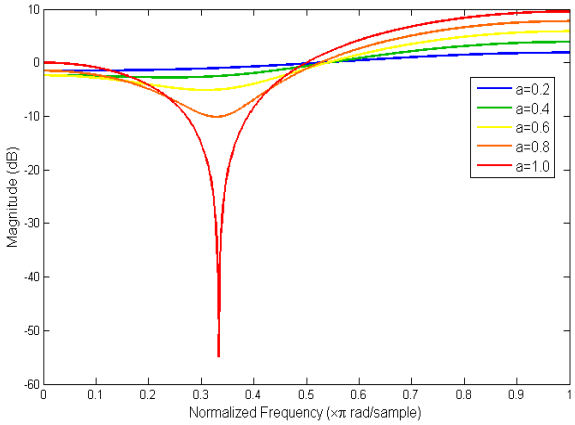

Fig. 2 Frequency responses of the three-coefficient ANF.

where ω_0 is the jammer frequency which specifies the place of the notch. The effect of the parameter a on the filter frequency response is illustrated in Fig.2.

The calculation of the parameter a is based on the maximizing of the receiver SNR:

$$SNR_0=\frac{(E\{y\})^2}{\sigma_y^2}=\frac{L^2h_0^2}{L(1+\sigma_n^2)\sum_{k=0}^{N} h_k^2-Lh_0^2+\sigma_{j0}^2} \quad (11)$$

where y is the output of the receiver correlator and σ_{j0} is the power of the jamming at the output of correlator. h_k for k=1, 2, ..., N are the notch filter coefficients which are extracted from the filter impulse response:

$$h(n)=\delta(n)-(2a\cos\omega_0)\delta(n-1)+a^2\delta(n-2) \quad (12)$$

Therefore, the coefficients of the discussed ANF are $h_0=1$, $h_1=-2a\cos(\omega_0)$, and $h_2=a^2$. Considering a single CWI in the form of Eq. (9), the power of jamming signal at the correlator output is calculated as [17]:

$$\sigma_{j0}^2 \approx LA^2(1-a)^2\left(\frac{1}{2}+\frac{a^2}{2}-a\cos2\omega_0\right) \quad (13)$$

Therefore, the output SNR of the described three coefficients ANF in the presence of a single CWI is defined as:

$$SNR_0=\frac{L}{(1+\sigma^2)(1+a^4+4a^2\cos^2\omega_0)-1+A^2(1-a)^2\left[\frac{1}{2}+\frac{a^2}{2}-a\cos2\omega_0\right]} \quad (14)$$

If we write the denominator of Eq. (14) as the function of a, then the optimum value of a which can be calculated from $f'(a) = 0$ leads to the maximum SNR.

3.3 WP Based Mitigation Algorithm

In the proposed mitigation system (which will be introduced later), the WP based mitigation algorithm has two main roles: first, removing the remaining

jamming effects and second, de-noising. It can be classified in four steps:

Step1: Wavelet decomposition. Choose mother wavelet function, the number of decomposition levels *L*, and then decompose the signal *S(k)* to *L* stages WP.

Step2: Selection of optimal tree (i.e. determination of the best WP basis in order to have the best interference rejection). The most suitable decomposition of a given signal can be chosen with respect to an entropy-based criterion. There are several entropies and the 'Shannon' entropy criterion is employed in this paper.

Step3: WP coefficients thresholding. Select the appropriate threshold which depends on the noise and the jamming levels and apply it at each decomposition level.

Step4: WP reconstruction. According to the *Lth* low and high frequency wavelet coefficients, the reconstruction of WP is accomplished.

The WP based mitigation algorithm is formulized as:

$$z=WP(y) \tag{15}$$

$$t=T(z,thr) \tag{16}$$

$$\text{desired signal}=WP^{-1}(t)=WP^{-1}oToWP(y) \tag{17}$$

where *WP* and *WP-1* denote WPT and inverse WPT operators and *T* is the thresholding operator with threshold *thr*. *T* determines the type of thresholding (soft or hard thresholding). Selection of the threshold is the most important step among these four steps.

3.3.1 Proposed Threshold Selection Method

Usually *thr* is selected with respect to the noise level σ^2 (e.g. $thr = 4\sigma$ is a common choice). However, this paper proposes a thresholding technique based on the optimization of universal thresholding:

$$thr=\gamma\sqrt{2\ln(N\ln(N))/\ln(2)} \tag{18}$$

where, *N* is the length of signal. γ is standard deviation defined as:

$$\gamma=\frac{MAD}{0.6745} \tag{19}$$

where, MAD is the median absolute deviation of the wavelet coefficients (in the case of noisy signal $\gamma=\sigma$). By using median, we can approximately achieve a good estimation from added white noise to the signal. But when the signal is contaminated by interference or when the SNR value is small, using median increases the probability of noise existence. Therefore, we employ Average Absolute Deviation (AAD) standard to optimize universal thresholding for anti-jamming applications:

$$AAD(c_i)=mean(|c_i|) \tag{20}$$

where, c_i represents the wavelet coefficients on a given band *i*. This threshold calculation method is quick and simple and does not require complex calculations.

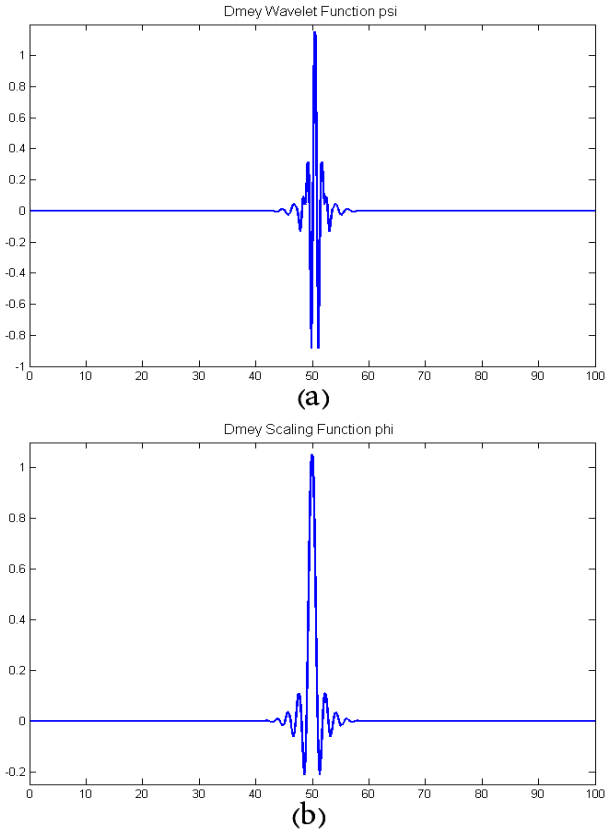

Fig. 3 'Dmey' filter (a) Wavelet function and (b) scaling function.

Moreover, optimum *thr* values are calculated according to different kinds of jamming and JSR values and they are saved in a memory. They will be used in a right time.

3.3.2 Selection of the Mother Wavelet, Wavelet Filter Length and the Decomposition Level

The choice of mother wavelet function is accomplished according to its maximum resemblance to the desired signal (jamming signal). Increasing the length of the wavelet filter causes the reduction of the side lobe and then improves the acquisition performance. Such effect is evident for smaller values of decomposition levels. In theory, as the number of decomposition levels increases, the resolution of the elimination frequency bands, the time of calculation and the complexity of implementation increase, too. Frequency specifications of the mother wavelet, jamming and GPS signal, has a significant impact on the decomposition depth selection. An optimum decomposition depth selection can make a good trade-off between algorithm performance and implementation complexity. In this paper, the number of decomposition level L is set to $L = 7$ and the discrete Meyer ('Dmey') wavelet with length of 102 is selected as the mother wavelet. In Fig. 3, wavelet and scaling function of 'Dmey' filter is depicted.

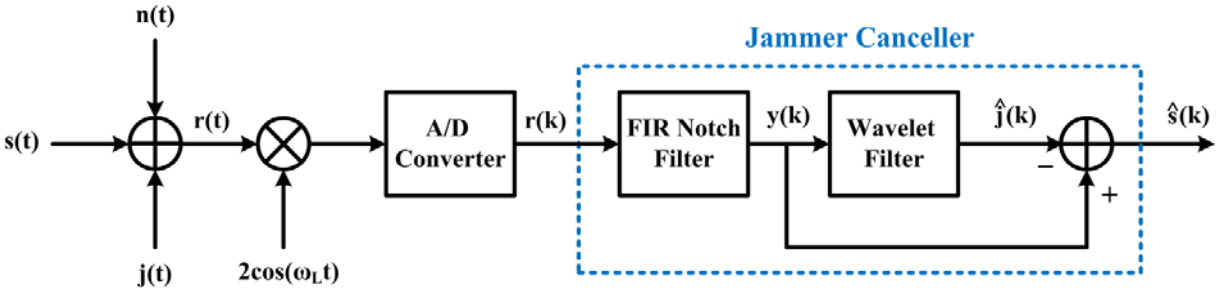

Fig. 4 Block diagram of the GPS anti-jamming system.

3.4 Proposed Cascade Filter

In the CWI rejection applications, notch filter is preferred due to its precise frequency adjustment regarding the WPT based filtering methods. The three coefficient FIR notch filter was studied in section 3.2. This filter can be easily designed and implemented in a GPS receiver. However, for high power jammers, the optimum value of parameter a (depth of notch) increases until it reaches to one. This wide and deep notch filter generates self-noise and causes reduction in the receiver SNR. To overcome the disadvantage of these filters, we propose a cascade form of ANF and wavelet filter for the jamming suppression applications. A simplified block diagram of the proposed cascade filter is illustrated in Fig. 4. Indeed, the novelty of the proposed anti-jamming system is employing (cascading) two filters that can cover each other drawbacks. The ANF prevents wavelet filter to employ several decomposition levels (prevents computational load growth). The wavelet filter prevents ANF to select a deep notch for jamming mitigation (prevents SNR reduction).

The aim of the jammer canceller (cascade filter) is to retrieve original signal *s(k)* and the output of the cascade filter is an estimation of the signal $\hat{s}(k)$. The received signal is first processed through the ANF. The input of the ANF is the digital version of contaminated received signal *r(k)*.

It is depicted in Fig. 4 that the second block of the cascade filter is the wavelet filter. The wavelet filter has two tasks: jamming rejection and de-noising. The input of this block is *y(k)*. In this block, the jammer (or the jammer+noise) is estimated in the de-noising procedure instead of the GPS signal (J (or $J+n$) is desired signal). The power of the received GPS signal is about *-160 dBW* (*22 dB* less than the noise power) and the observation would be dominated by the noise and jamming. Hence, in the second block the jamming signal *j(k)* is estimated and then it is removed from the contaminated signal:

$$\hat{J}=WP^{-1}oToWP(y) \tag{21}$$

$$\hat{s}=y-\hat{J}=y-WP^{-1}oToWP(y)=(I-WP^{-1}oToWP)(y) \tag{22}$$

where, I is the identity operator and $WP^{-1}\circ WP = I$. Therefore, Eq. (22) can be rewritten as:

$$\hat{s}=WP^{-1}oT^{s}(\text{or } T^{h})oWP(y) \tag{23}$$

$$T^{s}(c)=c-T_{Soft}(c)=\begin{cases} c\text{-sign}(c)(\|c\|-thr) & \text{if } \|c\|\geq thr \\ c & \text{otherwise} \end{cases} \tag{24}$$

$$T^{h}(c)=c-T_{Hard}(c)=\begin{cases} 0 & \text{if } \|c\|\geq thr \\ c & \text{otherwise} \end{cases} \tag{25}$$

where, c denotes the wavelet coefficients. $T^{s}(c)$ is calculated based on soft-thresholding operator $T_{Soft}(c)$. $T^{h}(c)$ is calculated based on hard-thresholding operator $T_{Hard}(c)$ [14]. The retrieved signal $\hat{s}$ is free from jammer and noise and it can be processed by the acquisition and tracking units of the GPS receiver.

The jamming rejection process of the second block is done by a subtraction. So, this process needs storage of the received signal and also fine synchronization procedure. However, the WPT algorithm can be implemented as a plug-in filter in the GPS receiver. Moreover, thanks to recent digital signal processors, the proposed cascade filter is a practical real-time anti-jamming system for GPS receivers.

It must be noted that the concept of recent WPT-based works [12, 13] is based on removing interfered sub-bands which have two main drawbacks: (a) when the jamming lies in several sub-bans, a large portion of the signal will remove by removing all interfered sub-bands (b) furthermore, when a small part of interference lies in a sub-band, removing the entire of that sub-band causes inaccurate signal reconstruction. The concept of the employed WP-based algorithm is based on thresholding the interfered sub-bands [14]. So, when a part of interference lies in a sub-band, the entire of that sub-band will not be removed.

4 Experimental Results

A test setup is developed for the performance evaluation of the proposed anti-jamming algorithm in various conditions (Fig. 5). It consists of a GPS antenna, a GPS receiver, an RF signal generator, a spectrum analyzer, a combiner and a computer.

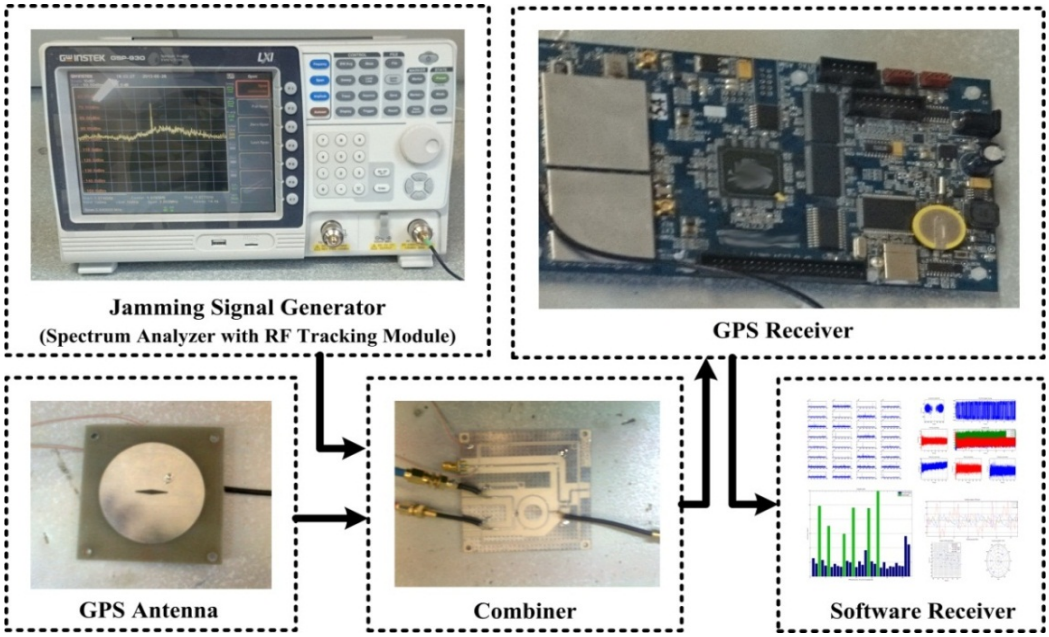

Fig. 5 Test setup.

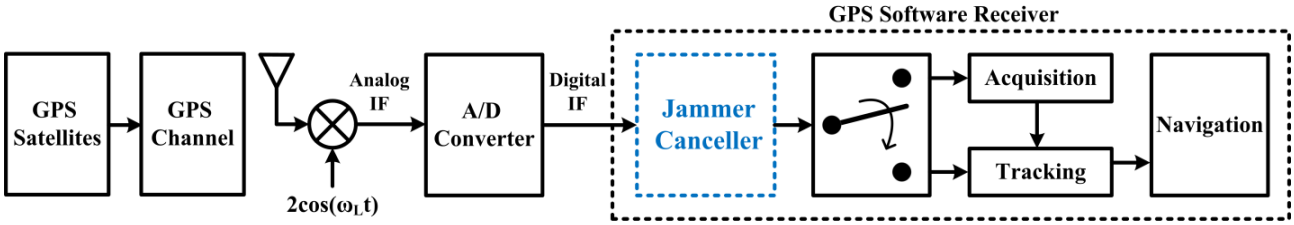

Fig. 6 Position of the jammer canceller in the GPS receiver.

Jamming signal generated in RF signal generator is combined with the real recorded GPS signal in the combiner. The combined signal is processed in the GPS receiver front-end and the output of the analogue to digital converter of the receiver is fed to the GPS software receiver. The use of a software receiver can accelerate acquisition, tracking and navigation processes. Furthermore, several jamming scenarios (that are not easy to implement in practice) can be designed and tested in the computer (the software receiver). The jammer canceller is also implemented in the GPS software receiver as depicted in Fig. 6.

Two different data sets are provided for the performance examination of the proposed rejection filter: first, real recorded GPS data combined with simulated jamming signal and second, real recorded GPS data combined with real jamming signals. Simulation parameters are shown in Table 1. The GPS signal that is saved in a test interval contains N = 62854 samples.

The performance of the proposed filter is expressed in terms of the number of acquired satellites, acquisition metric α_{max}, SNR gain and Mean Square Error (MSE) of the IF estimation.

Table 1 Parameters of simulation.

Parameter	Value
Desired signal	GPS L1 C/A code
Sampling frequency f_s	5.7143 MHz
Intermediate frequency f_{IF}	1.405 MHz
Signal bandwidth	2.046 MHz
Bits of A/D-quantization levels	2 bits-4 levels
PLL noise bandwidth	25 Hz
DLL noise bandwidth	2 Hz
DLL and PLL damping ratio	0.7

The purpose of the acquisition unit is to find the signal parameters for all the available satellites. The acquisition function looks for a GPS signal in frequency steps of 0.5 KHz. The acquisition metric is defined as:

$$\alpha_{\max} = \frac{R_1}{R_2} \tag{26}$$

where α_{max} represents the ratio between the highest correlation peak R_1 and the second highest correlation peak R_2 in the search space for each channel. This ratio is compared to the threshold value which is preset in the receiver.

The SNR gain (SNR improvement) is the difference of the $SNR_{out,dB}$ and $SNR_{in,dB}$. The *in* and *out* indexes refer to the input and output signals of the jammer canceller, respectively.

$$\text{SNR gain}=\frac{E\left(\left|y_k - s_k\right|^2\right)}{E\left(\left|\hat{s}_k - s_k\right|^2\right)} \tag{27}$$

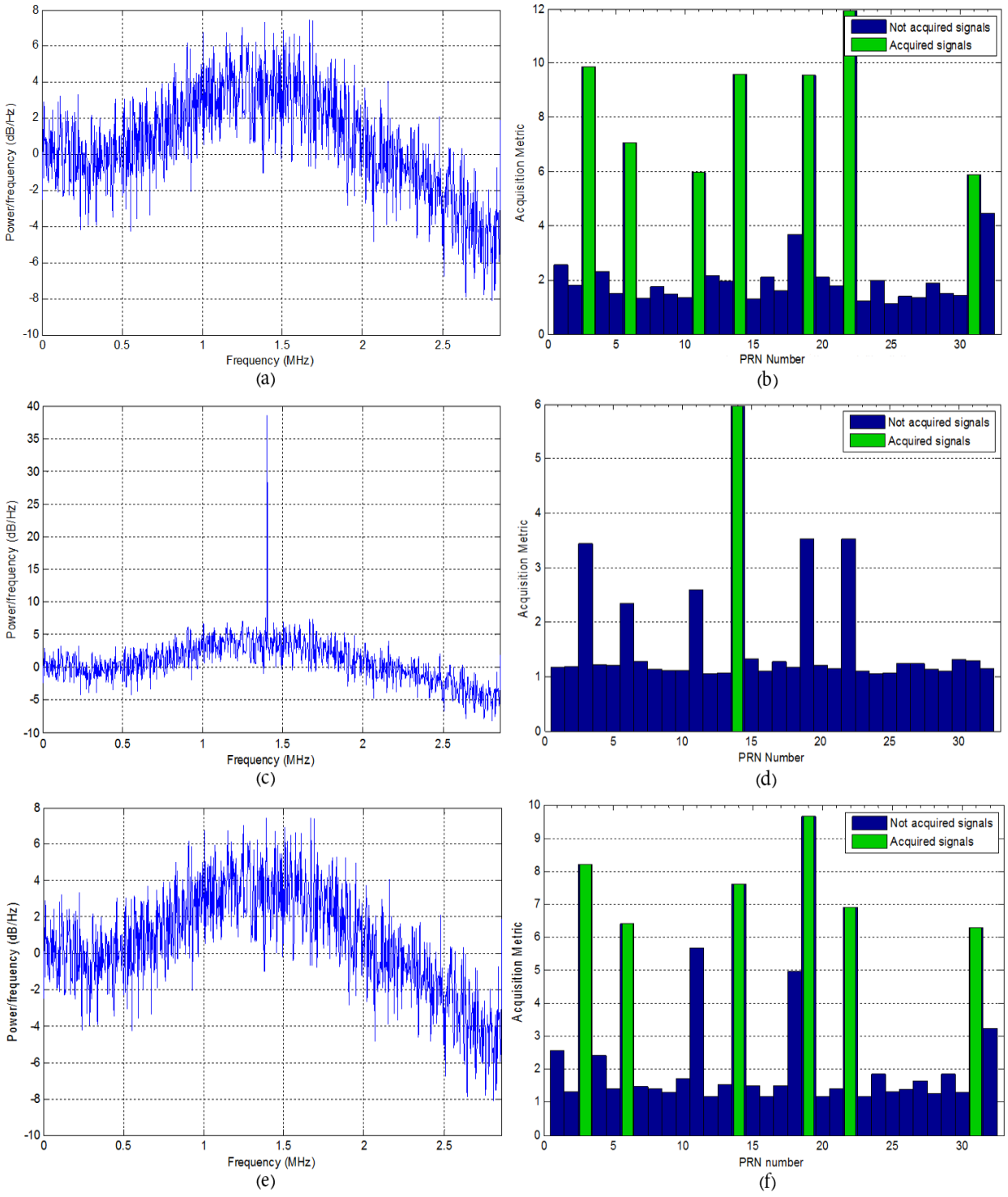

Fig. 7 (a) PSD of the received GPS plus noise signal (without jammer), (b) acquisition results of the received GPS plus noise signal (without jammer), (c) PSD of the jammed signal (simulated SCWI, JSR = 50 dB), (d) acquisition results of the jammed signal (simulated SCWI, JSR = 50 dB), (e) PSD of the estimated signal (simulated SCWI), and (f) acquisition results of the estimated signal (simulated SCWI).

In the Eq. (27), E is the expectation operator, $\hat{s}$ is the jammer free signal estimated by the jammer canceller and s is the uncontaminated GPS signal.

MSE represents the similarity between the original signal and the retrieved signal:

$$MSE=\frac{1}{N}\sum(\hat{s}-s)^2 \quad (28)$$

As mentioned earlier, N is the length of the signal. The smaller value of MSE indicates that the retrieved signal is a better approximation of the original signal.

4.1 First Data Set

It was mentioned before that the first data set is composed of the real recorded GPS signal and the simulated jamming signal. The JSR of the Single-Tone CWI (SCWI) and MCWI is changed in the range of 40-65 *dB*. It is calculated as:

$$JSR=10\log\frac{J}{S} \quad (29)$$

where J is the jammer power and S is the GPS signal power.

The employed SCWI is a pure sinusoidal signal located in the main lobe of the GPS signal (0.4-2.4 MHz). The Power Spectral Density (PSD) of the received, contaminated and retrieved signals and the acquisition results (the number of acquired satellites) are shown in Fig. 7.

It is illustrated in Fig. 7-c that an SCWI (JSR = 50 dB) can decrease the number of acquired satellites to only one satellite which is insufficient for navigation. Therefore, a jammer canceller should be employed to reject the jamming signals and retrieve the lost satellites. Fig. 7-e and Fig. 7-f show that the proposed jammer canceller rejected the SCWI and retrieved six satellites. The acquisition metric α_{max} is calculated for the wavelet-based jammer canceller [14], the notch filter [17] and the proposed jammer canceller for different JSRs of an SCWI (Fig. 8).

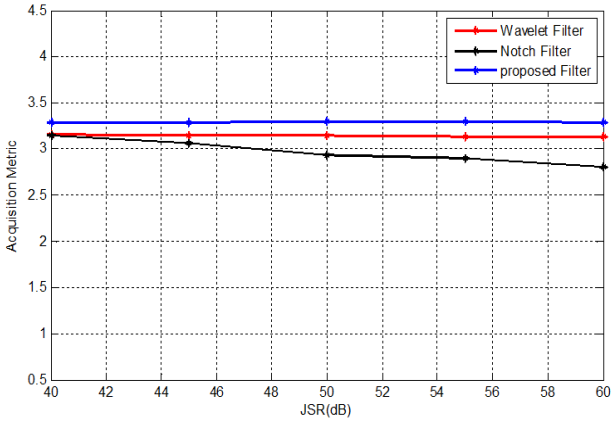

Fig. 8 Acquisition metric vs. JSR for the estimated signal (simulated SCWI).

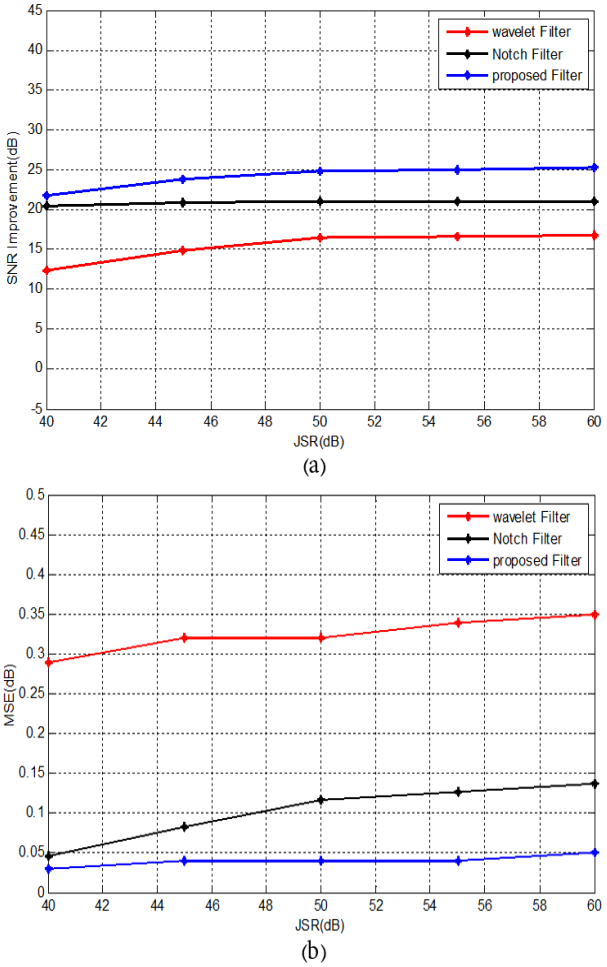

Fig. 9 (a) SNR improvement vs. JSR for the estimated signal (simulated SCWI), and (b) MSE vs. JSR for the estimated signal (simulated SCWI).

Fig. 8 shows that the α_{max} of the signal which is retrieved by the proposed filter has a greater value respect to the α_{max} of the signals which are retrieved by the wavelet and the notch filters. It is demonstrated that the proposed filter can better retrieve the lost satellites respect to the wavelet [14] and notch filters [17].

The SNR gain and MSE of the retrieved GPS signals are presented in Fig. 9. This figure also compares the performance of the proposed, wavelet only [14] and notch only [17] filters in terms of SNR gain and MSE.

Fig. 9 illustrated that the performance of the notch filter [17] is close to the proposed filter in the low values of JSR. In the high values of JSR the self-noise of the notch filter degrades its anti-jamming performance. The proposed filter overcomes this issue by employing a WPT-based filter.

In order to evaluate the performance of the proposed filter for the case of MCWI rejection, Tables 2, 3 and 4 are presented.

Table 2 Acquisition metric of the proposed cascade filter, ANF and wavelet filter (simulated MCWI).

JSR (dB)	Wavelet Filter [14]	Notch Filter [17]	Proposed Filter
45	2.97	3	3.24
50	2.99	2.92	3.10
55	2.51	2.85	2.92
60	2.48	2.82	2.90
65	2.52	2.87	2.86

Table 3 SNR gain of the proposed cascade filter, ANF and wavelet filter (simulated MCWI).

JSR (dB)	Wavelet Filter [14]	Notch Filter [17]	Proposed Filter
45	13.13	21.55	22.61
50	15.98	23.48	24.15
55	16.40	23.89	24.91
60	16.61	24.05	25.17
65	17.61	22.56	22.48

Table 4 MSE of the proposed cascade filter, ANF and wavelet filter (simulated MCWI).

JSR (dB)	Wavelet Filter [14]	Notch Filter [17]	Proposed Filter
45	0.74	0.10	0.08
50	0.76	0.13	0.11
55	1	0.17	0.14
60	1.04	0.18	0.14
65	0.9	0.28	0.29

Table 2 and Fig. 8 show that in term of the acquisition metric, proposed filter has an average improvement of 8%, 7% over the wavelet filter [14] and ANF [17], respectively. Table 3 and Fig. 9-a indicate that in term of the SNR gain, the proposed cascade filter have an average progress of 53% and 9% over the wavelet filter [14] and ANF [17], respectively. Table 4 and Fig. 9-b emphasize that in term of the MSE, the proposed filter have an average improvement of 85%, 37% over the wavelet filter [14] and ANF [17], respectively.

4.2 Second Data Set

The second data set is composed of the real recorded GPS signal which is contaminated by real jamming signal. The jamming signal is created by an RF signal generator. Fig. 10 shows the PSD of the GPS signal and acquisition results of the receiver in the presence of a real MCWI. It also illustrates the PSD and acquisition results of the retrieved signal.

Fig. 10-a depicts that no satellite can be acquired by the receiver in the presence of real MCWI (JSR = 55 dB). However, Fig. 10-d shows that the proposed jammer canceller can retrieve five satellites which are sufficient for the navigation.

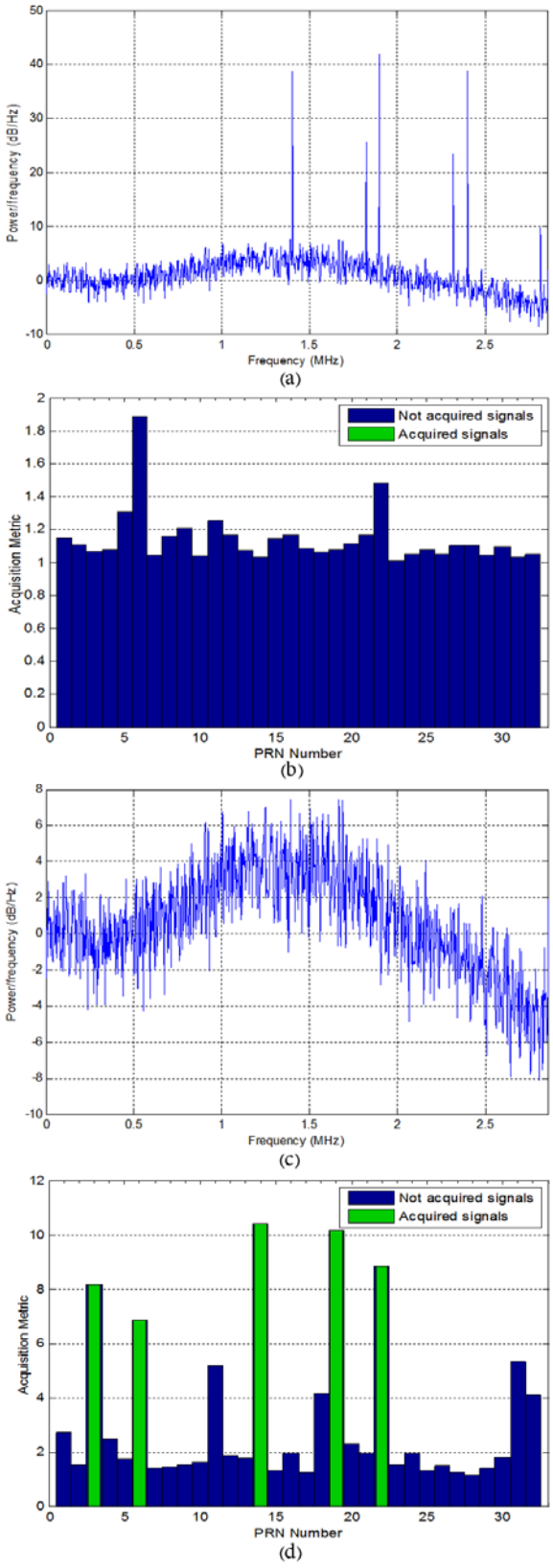

Fig. 10 (a) PSD of the jammed signal (real MCWI, JSR=55 dB), (b) acquisition results of the jammed signal (real MCWI, JSR=55 dB), (c) PSD of the estimated signal (real MCWI), and (d) acquisition results of the estimated signal (real MCWI).

Fig 10-c illustrates that the proposed filter removed all the jamming signals from the GPS signal spectrum. The acquisition metric α_{max} is presented in Fig. 11 for the range of 45-65 dB JSR values.

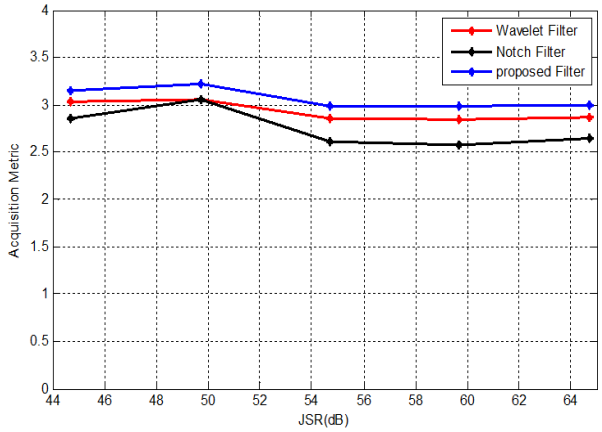

Fig. 11 Acquisition metric vs. JSR for the estimated signal (real MCWI).

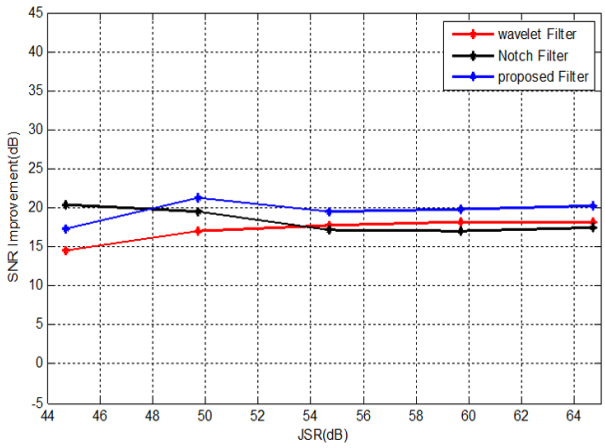

(a)

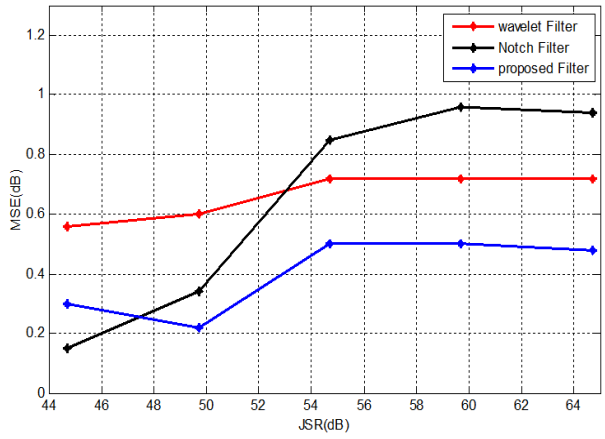

(b)

Fig. 12 (a) SNR improvement vs. JSR for the estimated signal (real MCWI), (b) MSE vs. JSR for the estimated signal (real MCWI).

Fig. 11 demonstrates that the proposed filter can better acquire satellites compared to the ANF [17] and the wavelet filter [14]. The SNR gain and MSE for the estimated signal by the proposed filter, ANF and the wavelet filter are presented in Fig. 12.

Fig. 12 shows that the proposed filter outperforms the ANF [17] and the wavelet filter [14] in terms of SNR gain and MSE. However, the ANF has a better performance for the JSR value lower than 48 dB due to the negligible self-noise of the ANF in these JSR values. The performance of the proposed filter, ANF and wavelet filter in the case of SCWI rejection are compared in the Tables 5, 6 and 7.

Table 5 and Fig. 11 show that in term of the acquisition metric, the proposed filter has an average improvement of 3%, 11% over the wavelet filter [14] and ANF [17], respectively. Table 6 and Fig. 12-a indicate that in term of the SNR gain, the proposed filter has an average progress of 31% and 9% over the wavelet filter [14] and ANF [17], respectively. Table 7 and Fig. 12-b emphasize that in term of the MSE, proposed filter has an average progress of 58%, 26% over the wavelet filter [14] and ANF [17], respectively.

Table 5 Acquisition metric of the proposed cascade filter, ANF and wavelet filter (real SCWI).

JSR (dB)	Wavelet Filter [14]	Notch Filter [17]	Proposed Filter
40	3.09	3.14	3.21
45	3.21	3.02	3.17
50	3.09	2.78	3.16
55	3.08	2.73	3.14
60	3.04	2.66	3.09

Table 6 SNR gain of the proposed cascade filter, ANF and wavelet filter (real SCWI).

JSR (dB)	Wavelet Filter [14]	Notch Filter [17]	Proposed Filter
40	10.65	19.77	20.82
45	14.96	18.29	19.72
50	14.81	18.99	21.23
55	15.63	18.72	21.10
60	15.90	18.65	21.17

Table 7 MSE of the proposed cascade filter, ANF and wavelet filter (real SCWI).

JSR (dB)	Wavelet Filter [14]	Notch Filter [17]	Proposed Filter
40	0.47	0.05	0.04
45	0.32	0.15	0.10
50	0.49	0.18	0.12
55	0.45	0.22	0.12
60	0.45	0.24	0.13

5 Conclusion

In this paper, a cascade three-coefficient ANF with an adaptive WPT-based filter was proposed for CWI suppression. In the first step, the jamming signal was mitigated by a simple FIR filter. To overcome the receiver performance degradation due to the self-noise effect of the FIR filter, the remaining jamming effects and also the noise of the notch filter was rejected by a WPT-based filter in the second step. The main advantage of the WPT-based filter is that it does not require the knowledge of the interference instantaneous frequency. The cascade filter presented considerable improvement in the jamming mitigation process for higher JSR values. It was well-suited for low cost applications because of its applicability on low cost processors. The proposed method was applied to two experimental data sets: the simulated jammer and the real jammer, which are added to the real recorded GPS signals. The results showed that the cascade filter has an average progress of 42%, 71%, and 6% over WPT-based filter in terms of SNR gain, MSE and acquisition metric, respectively. It has an average progress of 9%, 31%, and 9% over ANF in terms of SNR gain, MSE and acquisition metric, respectively.

Acknowledgment

The authors would like to thank Iran National Science Foundation Science deputy of presidency for their valuable support during the authors' research work.

References

[1] N. Ward and R. Johannessen, "Interference to GPS in the Marine Environment", *Journal of Navigation*, Vol. 49, No. 2, pp. 210-218, 1996.

[2] J. R. Sklar, "Interference Mitigation Approaches for the Global Positioning System", *Lincoln Laboratory Journal*, Vol. 14, No. 2, pp. 167-180, 2003.

[3] D. Borio, "GNSS Acquisition in the Presence of Continuous Wave Interference", *IEEE Trans. on Aerospace and Electronic Systems*, Vol. 46, No. 1, pp. 47-60, 2010.

[4] F. A. Khan, C. Rizos and A. G. Dempster, "Locata Performance Evaluation in the Presence of Wide- and Narrow-Band Interference", *Journal of Navigation*, Vol. 63, No. 3, pp. 527-543, 2010.

[5] M. Li, A. G. Dempster, A. T. Balaei, C. Rizos and F. Wang, "Switchable Beam Steering/Null Steering Algorithm for CW Interference Mitigation in GPS C/A Code Receivers", *IEEE Trans. on Aerospace and Electronic Systems*, Vol. 47, No. 3, pp. 1564-1579, 2011.

[6] W. Sun and M. G. Amin, "A Self-Coherence Anti-Jamming GPS Receiver", *IEEE Trans. on Signal Processing*, Vol. 53, No. 10, pp. 3910-3915, 2005.

[7] M. V. Tazebay and A. N. Akansu, "Adaptive Subband Transforms in Time-Frequency Excisers for DSSS Communications Systems", *IEEE Trans. on Signal Processing*, Vol. 43, No. 11, pp. 2776-2782, 1995.

[8] S. Savasta, L. Lo Presti and M. Rao, "Interference Mitigation in GNSS Receivers by a Time-Frequency Approach", *IEEE Trans. on Aerospace and Electronic Systems*, Vol. 49, No. 1, pp. 415-438, 2013.

[9] D. Borio, L. Camoriano, S. Savasta and L. Lo Presti, "Time-Frequency Excision for GNSS Applications", *IEEE Systems Journal*, Vol. 2, No. 1, pp. 27-37, 2008.

[10] M. J. Rezaei, M. Abedi and M. R. Mosavi, "New GPS Anti-Jamming System based on Multiple Short-Time Fourier Transform", *IET Radar, Sonar and Navigation*, DOI:10.1049/iet-rsn.2015.0417, 2016.

[11] T. H. Stitz and M. Renfors, "Filter Bank based Narrowband Interference Detection and Suppression in Spread Spectrum Systems", *EURASIP Journal on Applied Signal Processing*, Vol. 2004, pp. 1163-1176, 2004.

[12] L. Musumeci and F. Dovis, "Performance Assessment of Wavelet based Technique in Mitigating Narrow-Band Interference", *Proc. IEEE Int. Conf. on Localization and GNSS* (ICL-GNSS), pp. 1-6, 2013.

[13] E. Pardo, M. A. Rodriguez-Hernandez and J. J. Perez-Solano, "Narrowband Interference Suppression using Undecimated Wavelet Packets in Direct-Sequence Spread-Spectrum Receivers", *IEEE Trans. on Signal Processing*, Vol. 54, No. 9, pp. 3648-3653, 2006.

[14] M. R. Mosavi, M. Pashaian, M. J. Rezaei, and K. Mohammadi, "Jamming Mitigation in Global Positioning System Receivers using Wavelet Packet Coefficients Thresholding", *IET Signal Processing*, Vol. 9, No. 5, pp. 457-464, 2015.

[15] R. Wang, M. Yao, Z. Cheng and Z. Zou, "Interference Cancellation in GPS Receiver using Noise Subspace Tracking Algorithm", *Signal Processing*, Vol. 91, No. 2, pp. 338-343, 2011.

[16] A. V. Picois and N. Samama, "Near-Far Interference Mitigation for Pseudolites using Double Transmission", *IEEE Trans. on Aerospace and Electronic Systems*, Vol. 50, No. 4, pp. 2929-2941, 2014.

[17] M. G. Amin and C. Wang, "Optimum Interference Excision in Spread Spectrum Communications using Open-Loop Adaptive Filters", *IEEE Trans. on Signal Processing*, Vol. 47, No. 7, pp. 1966-1976, 1999.

[18] A. Giremus, J. Y. Turneret and A. Doucet, "A Fixed-Lag Particle Filter for Joint Detection/Compensation of Interference Effects in GPS Navigation", *IEEE Trans. on Signal*

Processing, Vol. 58, No. 12, pp. 6066-6079, 2010.

[19] M. R. Mosavi and F. Shafiee, "Narrowband Interference Suppression for GPS Navigation using Neural Networks", *GPS Solutions*, DOI: 10.1007/s10291-015-0442-8, 2015.

[20] D. Borio, L. Camoriano and L. Lo Presti, "Two-Pole and Multi-Pole Notch Filters: A Computationally Effective Solution for GNSS Interference Detection and Mitigation", *IEEE Systems Journal*, Vol. 2, No. 1, pp. 38-47, 2008.

[21] W. L. Mao, "Novel SREKF-Based Recurrent Neural Predictor for Narrowband/FM Interference Rejection in GPS", *Int. Journal of Electronics and Communications*, Vol. 62, No. 3, pp. 216-222, 2008.

[22] C. H. Kang, S. Y. Kim and C. G. Park, "Global Navigation Satellite System Interference Tracking and Mitigation based on an Adaptive Fading Kalman Filter", *IET Radar, Sonar and Navigation*, Vol. 9, No. 8, pp. 1030-1039, 2015.

[23] R. Vijayan and H. P. Poor, "Non-Linear Techniques for Interference Suppression in Spread-Spectrum Systems", *IEEE Trans. on Communications*, Vol. 38, No. 7, pp. 1060-1065, 1990.

[24] K. D. Rao and M. N. S. Swamy, "New Approach for Suppression of FM Jamming in GPS Receivers", *IEEE Trans. on Aerospace and Electronic Systems*, Vol. 42, No. 4, pp. 1464-1474, 2006.

Matin Pashaian received her B.Sc. degree in Electronic Engineering from Iran University of Science and Technology (IUST), Tehran, Iran, in 2011. She is currently a M.Sc. student in the Department of Electrical Engineering at IUST. Her research interests include signal processing and GPS security.

Mohammad Reza Mosavi received his B.Sc., M.Sc., and Ph.D. degrees in Electronic Engineering from Iran University of Science and Technology (IUST), Tehran, Iran, in 1997, 1998, and 2004, respectively. He is currently faculty member of Department of Electrical Engineering of IUST as professor. He is the author of more than 240 scientific publications on journals and international conferences. His research interests include circuits and systems design.

Maryam Salamat Moghaddasi received her B.Sc. degree in Electronic Engineering from Iran University of Science and Technology (IUST), Tehran, Iran, in 2011. She is currently a MSc. student in the Department of Electrical Engineering at IUST. Her research interests include GPS safety and signal processing.

Mohammad Javad Rezaei received his B.Sc., and M.Sc. degrees in Electronic Engineering from Iran University of Science and Technology (IUST), Tehran, Iran, in 2009, and 2011, respectively. He is currently a Ph.D. student in the Department of Electrical Engineering at IUST. His research interests include systems design, signal processing and GPS security.